



An approach to the question ‘How to account for human error in MAPOD?’

Martin Spies¹ and Hans Rieder¹

¹ Fraunhofer-Institute for Nondestructive Testing IZFP, Campus E3 1, 66123 Saarbrücken, Germany, martin.spies@izfp.fraunhofer.de

Abstract

To reduce the experimental efforts necessary for decent Probability of Detection (POD) studies, Model-Assisted POD (MAPOD) has evolved in recent years with efficient simulation techniques at hand to properly account for most of the relevant influencing inspection parameters. As in many industries manual UT is still high-valued, the human factor is one of the key issues for NDT reliability. Thus, the question has been raised how MAPOD can take these factors into account. We report on a first approach to this question. We compare POD-curves resulting from randomly manipulated datasets with the original MAPOD-curves and comment on the potential benefit of this approach.

1. Introduction

Progress in defect detection by using optimized or newly developed inspection techniques leads to improved reliability in NDT. In ultrasonic testing (UT) a reduction of human factors' influence can be achieved e.g. by replacing manual UT by mechanized scanning - if thoroughly applied. POD curves are popular and suitable tools to demonstrate and quantify the achieved improvements. The experimental efforts necessary for decent POD studies can be dramatically reduced by the MAPOD-approach [1] if efficient, validated simulation techniques are at hand. Thus, datasets can be generated which properly account for most of the relevant influencing inspection parameters such as material, component geometry and sensor properties. However, in many industries manual UT is still high-valued, thus the human factor being one of the key issues for NDT reliability. Accordingly, the question of how MAPOD can take human factor related issues into account needs to be addressed.

2. Consideration of human error in simulated datasets

In this contribution - as a first approach - we address the question how human error can be accounted for. Two main errors with considerable impact on the result of manual UT inspections are (1) missing out on a defect or not declaring an indication as a defect, and (2) assigning an erroneous signal amplitude to a defect by e.g. misreadings or a false calibration procedure. A straightforward approach to account for this in an \hat{a} -vs- \hat{a} -analysis is to correspondingly ‘manipulate’ certain data points by setting the amplitude to noise level (Case 1) or assigning a different amplitude (Case 2). In our approach we do this in a statistically random manner. In order to assign different amplitudes to a realistic amount of data points we refer to corresponding studies such as the PISC programme [2]. Here the efficiency of the inspectors in the detection of fatigue cracks



and lack of fusion defects was between 65% and 100%, most of the inspectors not reaching an efficiency of more than 80%. The synthetic datasets in our \hat{a} -vs- a -analysis are generated applying the Generalized Point Source Superposition technique and the MAPOD-curves are obtained using a Rayleigh-Rice statistical model (Ref. 3). Both are briefly described in the following with the main emphasis on the POD approach.

3. Probability of Detection – POD and MAPOD

3.1 Background

The experimental determination of POD curves requires well-defined inspection of appropriate test specimens. Here, not only the defect size to be detected is of importance, but also the material properties and the geometry of the components to be inspected. The POD curve (here determined as a function of defect size a) together with the relevant confidence intervals provides the defect size, which can be detected with a ‘reasonable’ probability. The principal shape of the POD curve shows that the Probability of Detection increases with defect size. At the size $a_{90/95}$ the lower 95% confidence bound hits the 90% POD level. The size $a_{90/95}$ is usually considered to be the securely detectable defect size in view of the requirements of component integrity [4].

For POD determination using an a -vs- \hat{a} -analysis test specimens supplied with model defects of different size are employed. In the inspection, a defect of size ‘ a ’ generates a signal of amplitude ‘ \hat{a} ’, which is interpreted as a hit, if it exceeds the decision threshold value \hat{a}_{dec} (e.g. 6 dB above noise). Assuming a specific statistical distribution of the measured data the resulting a -vs- \hat{a} -diagram can be transferred into a POD curve. The procedure described in MIL-HDBK-1823 uses the assumption that the signal amplitudes show a statistical normal distribution with constant variance. Also, a linear functional relation between amplitude ‘ \hat{a} ’ and defect size ‘ a ’ is assumed [4].

3.2 Rayleigh-Rice approach suitable for MAPOD calculations

In our approach we use a model for POD calculation which does not depend on these two assumptions. In the following, S designates the defect signal amplitude (corresponds to \hat{a}) and T designates the decision threshold (corresponds to \hat{a}_{dec}). We start with a defect signal amplitudes S_0 (e.g. calculated) which results in a signal amplitude S by superposition with statistical noise (‘white noise’, due to the inspection system and the material microstructure). Assuming that the noise is independent of the inspection position the noise signal N can be characterized by a mean noise amplitude N_0 [5, 6] (Fig. 1, left). The probability distribution for N with the variance σ_0 then results in the form of a Rayleigh-distribution according to [5]

$$P(N) = \frac{N}{\sigma_0^2} \exp \left[-\frac{N^2}{2\sigma_0^2} \right]$$

where $N_0 = \sigma_0\sqrt{\pi}/2$. The superposition of this noise with the defect amplitude signal S_0 leads to the total signal S with a Ricean probability distribution [5]

$$P(S) = \frac{S}{\sigma_0^2} \exp \left[-\frac{(S^2 + S_0^2)}{2\sigma_0^2} \right] I_0 \left(\frac{SS_0}{\sigma_0^2} \right)$$

where $I_0(x)$ designates the Bessel-function of order zero. The probability that S exceeds the threshold T follows according to

$$POD = \int_T^\infty P(S)dS$$

while the Probability of False Indication (PFI, i.e. the noise N exceeds the threshold T) is given by

$$PFI = \int_T^\infty P(N)dN$$

Thus, POD and PFI depend on the relationship of S_0 and N_0 to the decision threshold T (Fig. 1).

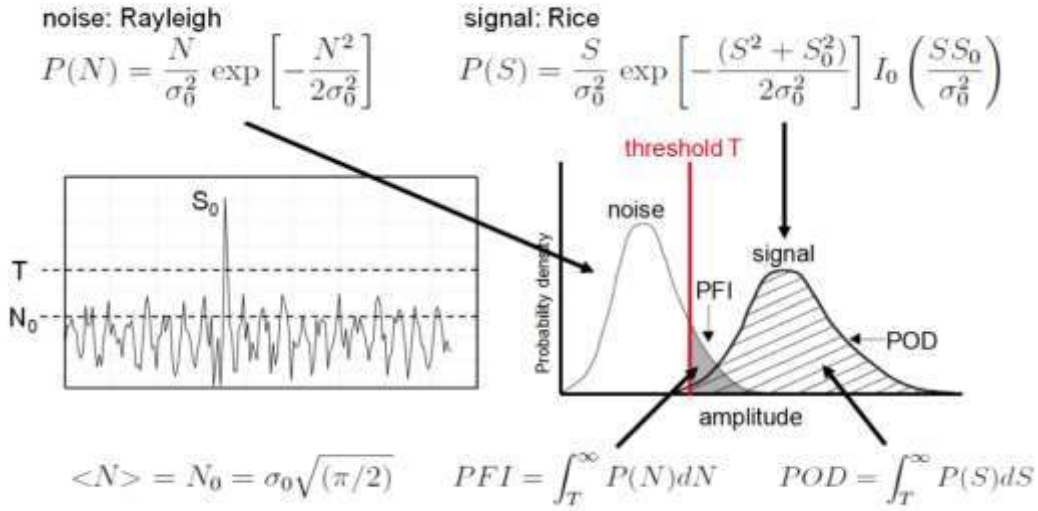


Figure 1. Schematic representation of the calculation procedure for POD and PFI in the Rayleigh-Rice model. The threshold T corresponds to \hat{a}_{dec} .

3.3 Simulation of defect signal amplitudes

The model-assisted POD determination relies on the calculation of defect amplitudes in simulated ('virtual') experiments. In our case, we use the Generalized Point Source Superposition technique [7, 8] which is based on a Rayleigh-Sommerfeld-type integral formulation. In a first step, the generation of ultrasonic waves by the transducer is simulated. In a second step, the interaction of the ultrasonic wave with a scattering defect is calculated on the basis of Kirchhoff-theory.

4. Example results and discussion

We address Case 1 and refer to a simulated dataset, validated against experimental data obtained on test block made of cast CuNiAl-bronze [3]. The test block had been

supplied with flat-bottomed holes of diameters ranging from 2 to 8 mm. Figure 2 shows the MAPOD-curve obtained from the original data as well as the MAPOD-curves obtained by randomly setting the amplitude values - originally above the decision threshold - of approx. one fifth (18.2%, referring to the average inspector performance as evaluated in the PISC study [2]) of the data points for the smaller defects (up to 5 mm diameter) to noise level. On the basis of five statistically varied datasets the value of $a_{90/95}$ indicated in Fig. 2 has been obtained as the average of the resulting MAPOD-curves. The human error thus introduced results in an increase of $a_{90/95}$ by about 0.5 mm, i.e. approx. 13%.

The POD curves shown in Figure 3 result from statistically increasing the number of missed defects to about one third (32.4%, referring to the poorest inspector performance as evaluated in the PISC study [2]). The average value of $a_{90/95}$ increases further, with the slope of the POD curve decreasing and the confidence bounds increasing.

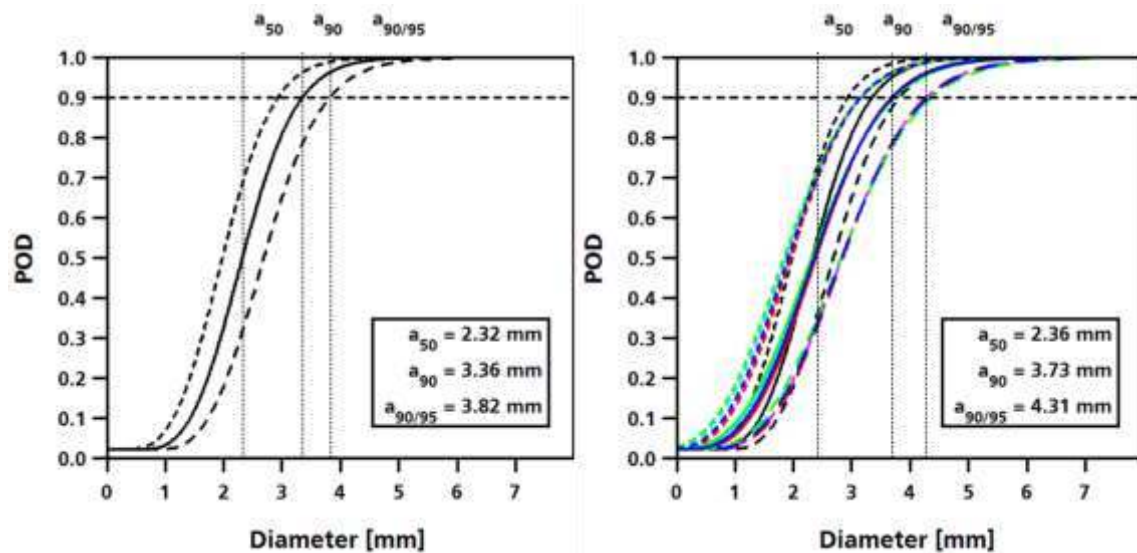


Figure 2. Left: MAPOD-curve (with confidence bounds) obtained for the original dataset (test block WB4); in the a -vs- \hat{a} -analysis a polynomial data fit has been used, rather than a linear log-log fit (as in Ref. 3). Right: five MAPOD-curves (coloured) obtained from statistically varied datasets setting 18.2 % of the signal amplitudes (up to 5 mm defects) to noise level.

5. Conclusion and outlook

We feel that this modified MAPOD approach leads to a more realistic reliability analysis if reliable information on inspector efficiency is available. In our study we have restricted the 'missing out on defects' to the smaller diameter model defects assuming that the largest defects will be securely detected. This, however, is not necessarily realistic in account of human error. If the large diameter defects will be included in the described procedure this would lead to larger changes in the variance of data points, while the results shown in Figs. 2 and 3 have been obtained on the basis of the valid assumption of constant variance $\sigma_0 = 4$ dB as determined from the original dataset. A variation of σ_0 with defect sizes will also have to be taken into account if we address Case 2 human error, i.e. statistically assigning different amplitudes to a certain percentage of the data points. Respective studies will follow in due course.

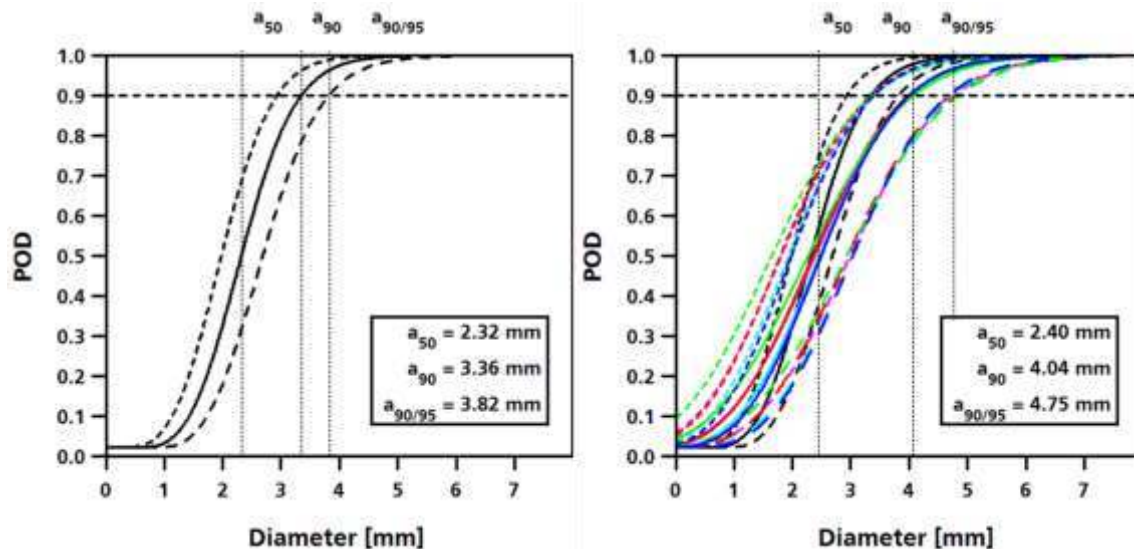


Figure 3. Left: MAPOD-curve (with confidence bounds) obtained for the original dataset (test block WB4, Ref. 3). Right: five MAPOD-curves (coloured) obtained from statistically varied datasets setting 32.4 % of the signal amplitudes (up to 5 mm defects) to noise level.

Acknowledgements

This work was elaborated within the joint research project ‘Reliability NDT’ within the Reactor Safety Research Program of the German Department of Economy and Energy (BMWi). The funding under Project Number 1501498B is gratefully acknowledged.

References

1. <http://www.cnde.iastate.edu/mapod/index.htm>
2. POD/POS curves for non-destructive examination - Offshore Technology Report, 2000/018. Prepared by Visser Consultancy Limited for the Health and Safety Executive (HSE).
3. M Spies, H Rieder and A Dillhöfer “Experimental and model-assisted POD-determination for volumetric defects in cast bronze components with various microstructures”, DGZfP Annual Meeting 2013, Proceedings BB-132, Di.1.C.1 (in German) .
4. DoD, 2009: Department of Defense Handbook Draft 2009; Nondestructive evaluation system reliability assessment; MIL-HDBK-1823, Draft 14 April 2009
5. J A Ogilvy “Model for predicting ultrasonic pulse-echo probability of detection”, NDT&E International 26, pp. 19-29, 1993.
6. S O Rice “Mathematical analysis of random noise”, Bell Syst. Tech. J24, pp. 46-156, 1945.
7. M Spies “Kirchhoff evaluation of scattered elastic wavefields in anisotropic media”, J. Acoust. Soc. Am. 107, pp. 2755-2759, 2000.
8. M Spies “Semi-analytical elastic wavefield modeling applied to arbitrarily oriented orthotropic media”, J. Acoust. Soc. Am. 110, pp. 68-79, 2001.